

Electrostatics of pyroelectric accelerators

T. Z. Fullem and Y. Danon^{a)}

Department of Mechanical, Aerospace and Nuclear Engineering, Rensselaer Polytechnic Institute, Troy, New York, USA

(Received 30 June 2009; accepted 16 August 2009; published online 2 October 2009)

Derivations for equations for calculating the potential and field strength in both single-crystal and two-crystal pyroelectric accelerators are presented. Such expressions for the single-crystal system are well established in the literature, but with cursory derivations. We provide a rigorous derivation of the single-crystal system and expand upon this physical understanding to derive expressions for the potential and field in a two-crystal system. The expressions are verified with finite element modeling and compared with experimental results. This allows for better understanding of pyroelectric accelerators. © 2009 American Institute of Physics. [doi:10.1063/1.3225916]

I. INTRODUCTION

Pyroelectric crystals can be used to generate a high potential to accelerate charged particles. Pyroelectric materials exhibit a nonzero spontaneous polarization (P) under equilibrium conditions and this polarization is a function of the material's temperature¹ as described by

$$\Delta P = \gamma \Delta T, \tag{1}$$

where γ is the pyroelectric coefficient ($176 \mu\text{C}/\text{m}^2 \text{K}$ for LiTaO_3)¹ and ΔT is the change in temperature. When a pyroelectric crystal experiences a change in temperature, the change in polarization creates an electric field that is strong enough to accelerate charged particles to energies on the order of hundreds of keV. Previous work has shown that this effect is strong enough to create compact sources of x-rays,²⁻⁴ electrons,⁵⁻⁷ ions,^{8,9} and neutrons (via D-D fusion).¹⁰⁻¹³

Pyroelectric crystals are often cut such that they have two faces normal to the axis of polarization. These faces are referred to as the Z^+ and Z^- faces. At room temperature, the spontaneous polarization of the Z^- face is negative, and the spontaneous polarization of the Z^+ face is positive. The pyroelectric effect causes the polarization to decrease during the heating of the crystal. If one were to heat the crystal while it was exposed to the atmosphere, free charges would accumulate on the crystal's surface so as to mask the change in polarization. In a vacuum, however, there are few free charges available and heating the crystal will result in an uncompensated positive charge on the Z^- surface (and an uncompensated negative charge on the Z^+ surface). The reverse effect occurs during cooling. The magnitude of this charge is given by

$$Q = A \gamma \Delta T, \tag{2}$$

where Q is the surface charge and A is the surface area. The increase in charge during the cooling phase creates an electric field. As the electric field strengthens, barrier tunneling can take place, causing electron emission from the Z^- surface during cooling.¹⁴

There are two common varieties of pyroelectric accelerators: single-crystal and two-crystal. In a single-crystal system, one face of the crystal is grounded and the other is electrically floating and faces a grounded target. The non-grounded surface and the target are separated by a vacuum gap or low pressure gas as shown in Fig. 1(a). In the two-crystal system, the grounded target is replaced by a second (and oppositely faced) crystal, as shown in Fig. 1(b). By oppositely faced, we mean that the Z^- face of one crystal faces the Z^+ face of the other crystal. Useful mathematical descriptions of the one-crystal system are available in the literature;¹¹ however, equations for the two-crystal system are not. A rigorous analysis of the one-crystal system will be provided and this analysis will be adapted to provide equations which can predict the potential and field in the gap of a two-crystal system.

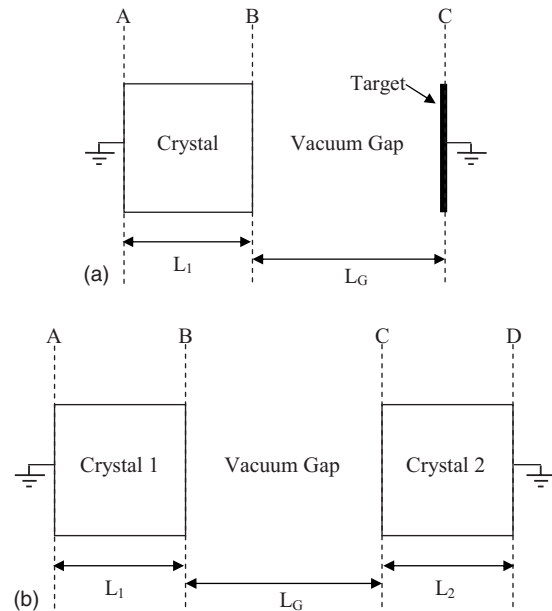


FIG. 1. (a) Sketch of a one-crystal system. (b) Sketch of a two-crystal system.

^{a)}Electronic mail: danony@rpi.edu.

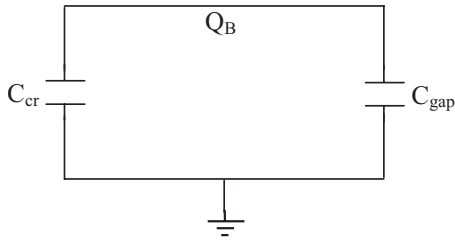


FIG. 2. The circuit diagram for the one-crystal system.

II. MATHEMATICAL ANALYSIS

A. One-crystal system

A sketch of a one-crystal pyroelectric accelerator is shown in Fig. 1(a). We define three planes (A, B, and C) in the figure. The crystal has been cut such that its axis of polarization is normal to planes A and B. In our experiments, we have used cylindrical crystals, which have been cut such that the cylinder's axis is parallel to the axis of polarization. The following derivations assume the same orientation of the axis; however, they are not confined to cylindrical crystals.

When the crystal in Fig. 1(a) experiences a temperature change, the total charge that develops on surface B (Q_B) is given by Eq. (2). As a result, a potential exists across the crystal and the gap and an electric field is also present. Consequently, if charged particles (such as electrons or ions) are present in the gap, they will be accelerated. The direction of the electric field in the gap (and the sign of the charge on surface B) is dependent on both the orientation of the axis of polarization (toward or away from B) and whether the crystal has been heated or cooled.

Since the crystal and the gap are both electrically insulating, this system can be modeled as two capacitors in parallel where surface B is common to both capacitors. The equivalent circuit is shown in Fig. 2. The equivalent capacitance (ignoring fringing fields) of this system is given by

$$C_{\text{eq}} = C_{\text{cr}} + C_{\text{gap}} = \frac{\epsilon_o \epsilon_{\text{cr}} A}{L_1} + \frac{\epsilon_o \epsilon_{\text{gap}} A}{L_G}, \quad (3)$$

where ϵ_o , ϵ_{cr} , and ϵ_{gap} are the permittivities of free space, the pyroelectric crystal, and the gap, respectively (if the gap is a vacuum, $\epsilon_{\text{gap}}=1$, however, we will leave this term in the equations for completeness). The potential across a capacitor is given by

$$V = \frac{Q}{C}. \quad (4)$$

Since C_{cr} and C_{gap} in Fig. 2 are in parallel, the potentials across both of these capacitors must be equal ($V_{\text{cr}}=V_{\text{gap}}$). Therefore, the potential across the gap is given by

$$V = \frac{Q_B}{C_{\text{eq}}} = \frac{A \gamma \Delta T}{\frac{\epsilon_o \epsilon_{\text{cr}} A}{L_1} + \frac{\epsilon_o \epsilon_{\text{gap}} A}{L_G}} = \frac{\gamma \Delta T}{\epsilon_o \left(\frac{\epsilon_{\text{cr}}}{L_1} + \frac{\epsilon_{\text{gap}}}{L_G} \right)}. \quad (5a)$$

In many cases $C_{\text{cr}} \gg C_{\text{gap}}$, therefore Eq. (5a) can be simplified as

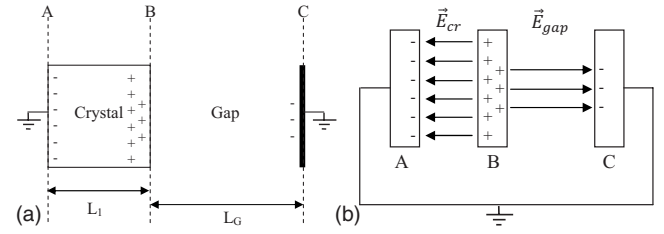


FIG. 3. (a) Sketch of the one-crystal system with example charges shown. The region containing the charges near plane B is substantially magnified. (b) Sketch of the equivalent capacitors of (a) showing a magnified view of the surfaces located on planes A, B, and C. Not to scale.

$$V \approx \frac{Q_B}{C_{\text{cr}}} = \frac{\gamma \Delta T L_1}{\epsilon_o \epsilon_{\text{cr}}}. \quad (5b)$$

The electric field strength in the gap is given by

$$E_G = \frac{V}{L_G} = \frac{\gamma \Delta T}{\epsilon_o \left(\frac{L_G \epsilon_{\text{cr}}}{L_1} + \epsilon_{\text{gap}} \right)}. \quad (6)$$

It should be noted that regarding the surface of the pyroelectric crystal as containing the “plate” of a capacitor (a conductor) is not a departure from reality since the resistivity of the surface of some pyroelectrics is lower than that of the bulk and exhibits metalliclike behavior.^{15,16}

We now have expressions for both the potential and field in the gap, and several papers on pyroelectric accelerators present the above equations in various forms. This is sufficient to analyze the one-crystal system. To aid in understanding the two-crystal system, however, some further analysis of the one-crystal system shall be conducted. It should be noted that the charge on surfaces A and C is not zero (even though these surfaces are grounded). When we say that a capacitor is charged with charge Q , this means that there is a charge $+Q$ on one plate and a charge $-Q$ on the other plate; therefore, the term Q in Eq. (4) implicitly refers to the absolute value of Q . The surface of the pyroelectric crystal at plane B can be thought of as containing two plates, one for capacitor C_{cr} and the other for capacitor C_{gap} . The total charge generated by the pyroelectric crystal (Q_B) divides itself among these two plates. The portion of charge Q_B that is associated with the crystal capacitor sees an equal and opposite charge (Q_A) on plane A (the grounded back of the crystal) and the other portion of the charge Q_B (which is associated with the gap capacitor) sees an equal and opposite charge (Q_C) on plane C (the grounded target). This is illustrated in Fig. 3. It is obvious that

$$Q_B = Q_A + Q_C. \quad (7)$$

It should be noted that Q_A and Q_C are not necessarily equal; rather their ratio is determined by the ratio of the capacitances of the gap and crystal,

$$V_{\text{cr}} = V_{\text{gap}} \Rightarrow \frac{Q_A}{C_{\text{cr}}} = \frac{Q_C}{C_{\text{gap}}} \Rightarrow \frac{Q_A L_1}{\epsilon_o \epsilon_{\text{cr}} A} = \frac{Q_C L_G}{\epsilon_o \epsilon_{\text{gap}} A}. \quad (8)$$

Using Eqs. (7) and (8), expressions for Q_A and Q_C can be derived.

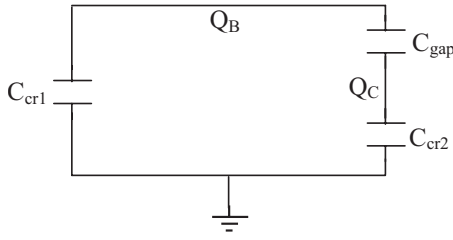


FIG. 4. A circuit diagram for the two-crystal system.

$$Q_A = \frac{Q_B}{1 + \frac{\epsilon_{\text{gap}} L_1}{\epsilon_{\text{cr}} L_G}}, \quad Q_C = \frac{Q_B}{1 + \frac{\epsilon_{\text{cr}} L_G}{\epsilon_{\text{gap}} L_1}}. \quad (9)$$

The veracity of Eqs. (8) and (9) can be verified by separately calculating the potentials across the crystal and the gap by using Eqs. (4) and (9) and the respective capacitances of the crystal and gap; both of these potentials are equivalent to Eq. (5a). Also of interest is the detailed discussion given by Pinto¹⁷ of the use of finite difference methods to determine electrostatic parameters for a geometry similar to that found in the one-crystal system.

B. Two-crystal system

To achieve a larger potential across the gap, it is possible to employ two oppositely faced crystals. By oppositely faced, we mean that the polarization axes of the two crystals are antiparallel. It is possible to face the crystals in the same direction of polarization, and the mathematical analysis below is valid for that case as well. Note that for crystals faced in the same direction, if the crystals are identical and experience identical temperature changes, the potential and field in the gap will be zero.

We can treat this as a system of three capacitors: C_{cr1} , C_{gap} , and C_{cr2} . When the crystals experience temperature changes, charges will develop on surfaces B and C and their magnitudes are given by

$$Q_B = A \gamma_1 \Delta T_1, \quad Q_C = A \gamma_2 \Delta T_2, \quad (10)$$

where the subscripts 1 and 2 denote the parameters for crystals 1 and 2, respectively. Be mindful of the signs of the charge (i.e., the orientation of the crystals.)

In Fig. 4, a circuit diagram is shown for the two-crystal system, analogous to that shown in Fig. 2 for the one-crystal system. Based on Fig. 4, one may be tempted to determine the potential across the gap by employing similar tactics to those used in Eqs. (3) and (5a). Namely, model the system as an equivalent capacitance (put the series combination of C_{gap} and C_{cr2} in parallel with C_{cr1}) and calculate the potential by inserting this and the charge generated by the pyroelectric crystals into Eq. (4). This will not work. Two capacitors in series can be replaced by their series equivalent combination if and only if the charge on both capacitors is the same. For the present arrangement, this would require $Q_C = 0$.

Figure 4, however, is not useless as it leads us to an expression which relates the potentials across the three capacitors,

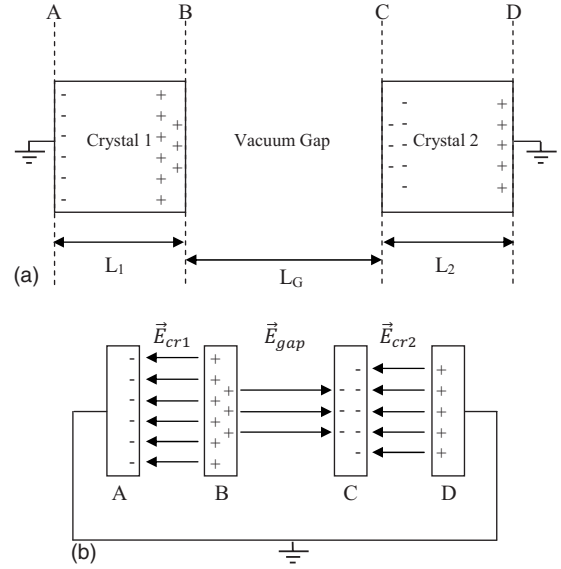


FIG. 5. (a) Sketch of a two-crystal system. The regions containing the charges near planes B and C are substantially magnified. (b) Sketch of the equivalent capacitors of (a) showing a magnified view of the surfaces located on planes A, B, C, and D. Not to scale.

$$V_{\text{cr1}} = V_{\text{gap}} + V_{\text{cr2}}, \quad (11)$$

where V_{cr1} , V_{gap} , and V_{cr2} are the potentials across the three capacitors shown in Fig. 4. The three capacitances are given by

$$C_{\text{cr1}} = \frac{\epsilon_0 \epsilon_{\text{cr1}} A}{L_1}, \quad C_{\text{gap}} = \frac{\epsilon_0 \epsilon_{\text{gap}} A}{L_{\text{gap}}}, \quad C_{\text{cr2}} = \frac{\epsilon_0 \epsilon_{\text{cr2}} A}{L_2}. \quad (12)$$

Equation (11) can be rewritten as

$$\frac{Q_1}{C_{\text{cr1}}} = \frac{Q_{\text{gap}}}{C_{\text{gap}}} + \frac{Q_2}{C_{\text{cr2}}}, \quad (13)$$

where Q_1 , Q_{gap} , and Q_2 are the charges on the respective capacitors. Note that Q_1 and Q_2 will be of opposite sign if the crystal axes are antiparallel.

In deriving expressions for the potential across the gap, it may aid in developing a physical understanding to draw a sketch of the charges and the field lines as was done in Fig. 3 for the one-crystal system; see Fig. 5.

The values of Q_B and Q_C are determined by the respective pyroelectric crystals and their temperature profiles in accordance with Eq. (10). As with the one-crystal system, some of the charge Q_B behaves as if it were the charge on capacitor C_{cr1} and the remainder behaves as if it were the charge on capacitor C_{gap} . Likewise, some of the charge Q_C behaves as if it were the charge on capacitor C_{cr2} and the remainder behaves as if it were the charge on capacitor C_{gap} . This can be expressed mathematically as

$$Q_B = Q_1 + Q_{\text{gap}}, \quad Q_C = Q_2 + Q_{\text{gap}}. \quad (14)$$

One may be tempted to write Eq. (14) with the absolute value of each term. This will work numerically, but is not physical; one must be careful to consider the three charge quantities as existing in the same physical location, consequently, they will all have the same sign.

Our objective is to find an expression for the potential across the gap. With Eq. (4) in mind and since the capacitance of the gap can be determined from the geometry of the system, what we need to find is an expression for Q_{gap} . Equations (13) and (14) form a system of three simultaneous equations [shown together as Eq. (15)], which, when solved, will yield an expression for V_{gap} (and V_{cr1} and V_{cr2}),

$$\begin{aligned} \frac{Q_1}{C_{\text{cr1}}} - \frac{Q_2}{C_{\text{cr2}}} - \frac{Q_{\text{gap}}}{C_{\text{gap}}} &= 0, \\ Q_2 + Q_{\text{gap}} &= Q_C, \\ Q_1 + Q_{\text{gap}} &= Q_B. \end{aligned} \quad (15)$$

The unknowns in this system of equations are Q_1 , Q_2 and Q_{gap} . All of the other parameters can be determined from the geometry of the system and material properties [Eqs. (10) and (12)]. Solving Eq. (15) yields the following:

$$Q_{\text{gap}} = \frac{-(Q_C C_{\text{cr1}} - Q_B C_{\text{cr2}}) C_{\text{gap}}}{(C_{\text{cr2}} C_{\text{cr1}} + C_{\text{cr2}} C_{\text{gap}} - C_{\text{cr1}} C_{\text{gap}})}, \quad (16)$$

$$V_{\text{gap}} = \frac{Q_{\text{gap}}}{C_{\text{gap}}} = \frac{-(Q_C C_{\text{cr1}} - Q_B C_{\text{cr2}})}{(C_{\text{cr2}} C_{\text{cr1}} + C_{\text{cr2}} C_{\text{gap}} - C_{\text{cr1}} C_{\text{gap}})}, \quad (17)$$

$$Q_1 = \frac{(Q_B C_{\text{cr2}} - Q_B C_{\text{gap}} + Q_C C_{\text{gap}}) C_{\text{cr1}}}{(C_{\text{cr2}} C_{\text{cr1}} + C_{\text{cr2}} C_{\text{gap}} - C_{\text{cr1}} C_{\text{gap}})}, \quad (18)$$

$$V_{\text{cr1}} = \frac{Q_1}{C_{\text{cr1}}} = \frac{(Q_B C_{\text{cr2}} - Q_B C_{\text{gap}} + Q_C C_{\text{gap}})}{(C_{\text{cr2}} C_{\text{cr1}} + C_{\text{cr2}} C_{\text{gap}} - C_{\text{cr1}} C_{\text{gap}})}, \quad (19)$$

$$Q_2 = \frac{(Q_C C_{\text{cr1}} - Q_B C_{\text{gap}} + Q_C C_{\text{gap}}) C_{\text{cr2}}}{(C_{\text{cr2}} C_{\text{cr1}} + C_{\text{cr2}} C_{\text{gap}} - C_{\text{cr1}} C_{\text{gap}})}, \quad (20)$$

$$V_{\text{cr2}} = \frac{Q_2}{C_{\text{cr2}}} = \frac{(Q_C C_{\text{cr1}} - Q_B C_{\text{gap}} + Q_C C_{\text{gap}})}{(C_{\text{cr2}} C_{\text{cr1}} + C_{\text{cr2}} C_{\text{gap}} - C_{\text{cr1}} C_{\text{gap}})}. \quad (21)$$

When using Eqs. (17), (19), and (21) to calculate potential, the appropriate signs for Q_B and Q_C must be inserted depending on the physical orientation of the respective crystals. For the case of identical antiparallel crystals that experience identical temperature profiles, the above equations can be simplified using

$$C_{\text{cr}} \equiv C_{\text{cr1}} = C_{\text{cr2}} \quad Q_{\gamma} \equiv Q_B = -Q_C, \quad (22)$$

which yields

$$V_{\text{gap}} = \frac{2Q_{\gamma}}{C_{\text{cr}}}. \quad (23)$$

Incorporating Eqs. (10) and (12) gives

$$V_{\text{gap}} = \frac{2Q_{\gamma}}{C_{\text{cr}}} = \frac{2\gamma\Delta TL_{\text{cr}}}{\epsilon_0\epsilon_{\text{cr}}}. \quad (24)$$

where $L_{\text{cr}}=L_1=L_2$ is the thickness of the two crystals. Note in Eq. (22), that if the polarization axes were parallel, $Q_B = Q_C$ which would give $V=0$.

III. VERIFICATION WITH FINITE ELEMENT ANALYSIS

The veracity of Eqs. (5a) and (17) can be assessed by calculating the potentials using numerical values of the parameters for typical systems and comparing this with the potentials calculated using finite element analysis of the corresponding systems. Finite element modeling was conducted with the COMSOL MULTIPHYSICS¹⁸ software package. We assume cylindrical LiTaO₃ pyroelectric crystals ($\gamma = 176 \mu\text{C}/\text{m}^2 \text{K}$ and $\epsilon_{\text{cr}}=46$)^{1,19} with a radius of 1 cm and a thickness of 1 cm, which experience $\Delta T=100 \text{ }^\circ\text{C}$. Furthermore, we shall assume that the gap is a perfect vacuum ($\epsilon_{\text{gap}}=1$) and has a length of 1.5 cm. For the one-crystal system, using the above values, Eq. (5a) (gives $V_{\text{gap}} = 426 \text{ kV}$; for the two-crystal system, using the above values, Eq. (24) gives $V_{\text{gap}}=864 \text{ kV}$. In both cases, finite element analysis agrees with these calculations to within 3%.

IV. COMPARISON WITH EXPERIMENTAL VALUES

The potential achieved in a pyroelectric accelerator can be measured by measuring the energy spectrum of the x-rays that are emitted due to the interaction of electrons that were accelerated across the gap with the objects that form the boundaries of the vacuum gap. This interaction results in characteristic x-ray peaks particular to the material with which the electrons collided and a continuous bremsstrahlung x-ray spectrum. The maximum energy of the x-ray continuum is indicative of the maximum electron energy and therefore the potential across the gap. Such measurements indicate¹² that the potential across the gap in the one-crystal system is $\sim 100 \text{ kV}$ and in the two-crystal system is $\sim 220 \text{ kV}$. This is roughly a quarter of what is predicted for the ideal systems using Eqs. (5a) and (24), such discrepancies have been noted in previous works^{20,21} as well. We shall now discuss several intricacies of a real system that are not accounted for in the idealized model, which may mitigate the accelerating potential.

Implicit in Eq. (2) is the assumption that the pyroelectric coefficient is constant over the temperature range of interest. In reality, this parameter is temperature dependent. When using the pyroelectric charge to calculate the potential in Eq. (5a) (and the potentials in the two-crystal system), we assume that the crystal has an electrical conductivity of zero. The resistivity of LiTaO₃ at room temperature²² is $\sim 10^{15} \Omega \text{ cm}$. A more detailed version of Eq. (5a) is given by Lui *et al.*,¹⁵ which accounts for the temperature dependence of γ and various charge leakage mechanisms; they present experimental data to verify their detailed equation and found that it gives a potential that is roughly 18% less than that predicted by Eq. (5a) at a temperature of $100 \text{ }^\circ\text{C}$.

Equation (5a) also predicts that potential should increase linearly with increasing crystal thickness. This relationship has been shown to be accurate²³ for crystal thicknesses less than 1 cm, however, increasing the thickness beyond 1 cm does not increase the potential.³ In these experiments, the heat source was in contact with only the grounded face of the crystal and the temperature was measured at this location as well. Due to the low thermal conductivity of LiTaO₃ ($\sim 4 \text{ W/m K}$) (Ref. 24) the exposed face of a thicker crystal does

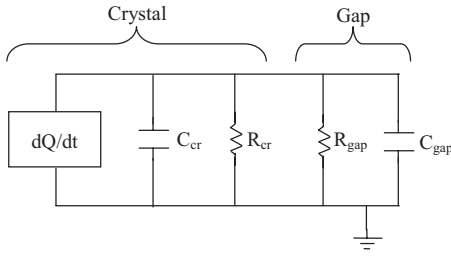


FIG. 6. Equivalent circuit showing the crystal and gap as lossy capacitors (Ref. 26).

not achieve as high of a temperature as the grounded face (whose temperature is being regulated.) For a 2 cm thick crystal, it was found²¹ that when the heated surface reached 110 °C, the exposed surface had reached a temperature of only 60 °C. It may be possible to overcome this problem by using a heating technique that heats the entire length of the crystal uniformly; however, such a technique would have to be noncontact (to avoid interfering the high potential surface). Noncontact heating techniques (i.e., radiative heating) are generally less efficient than contact methods.

The above analysis assumed that the crystal and gap were both ideal capacitors; while their conductivity is small, it is not zero. The crystal and the gap can be modeled as two lossy capacitors (the parallel combination of an ideal capacitor and a resistor) in parallel with an ideal charge generator, as shown in Fig. 6. Some charge will leak through each of the capacitors. This system is described by the following differential equation:

$$\frac{dq}{dt} = \gamma A \frac{dT}{dt} - \frac{V}{R_{cr}} - \frac{V}{R_{gap}} = \gamma A \frac{dT}{dt} - \frac{q}{C_{eq}} \left(\frac{1}{R_{cr}} + \frac{1}{R_{gap}} \right), \quad (25a)$$

where R_{gap} and R_{cr} are the resistances of the gap and the crystal, respectively, and C_{eq} is the equivalent capacitance of the gap and crystal ($C_{eq} = C_{gap} + C_{cr}$). This equation can be rewritten as

$$\frac{dV}{dt} = \frac{\gamma A}{C_{eq}} \frac{dT}{dt} - \frac{V}{R_{eq} C_{eq}}, \quad (25b)$$

where R_{eq} is the parallel combination of the crystal and gap resistances ($R_{eq}^{-1} = R_{gap}^{-1} + R_{cr}^{-1}$). Solutions to this equation are given by Lang and co-workers^{25,26} for several ranges of resistances and capacitances.

Determination of the resistance of the gap is not trivial. A rough estimate can be made by measuring the current of charged particles striking the target and the accelerating potential. For example, in one experiment, a current of 0.1 nA and a potential of 120 kV was measured⁹ across a 2 cm vacuum (for 1 cm thick, 0.5 cm diameter crystal), which gives a resistance of $\sim 10^{15} \Omega$. The gap in this system has been treated as a vacuum in the above analysis; however, it actually contains a low pressure (< 20 mTorr) fill gas (usually deuterium.) Since the fill gas can be ionized by the strong electric fields near the crystal and the ionization changes with time, the resistivity of the gas is not a fixed value. Furthermore, spontaneous discharges from the crystal to the ground have been observed at unpredictable intervals

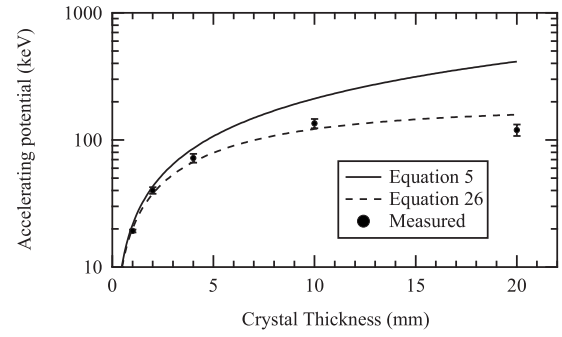


FIG. 7. Comparison of experimental data (Ref. 21) with the idealized model [Eq. (5a)] and with a model that accounts for charge leakage [Eq. (26)] for a one crystal system with a 5×5 mm² rectangular LiTaO₃ crystal using $\Delta T = 50$ °C, $R_g = 8 \times 10^{13} \Omega$, $\rho_{cr} = 10^{13} \Omega$ m, and $dT/dt = 0.5$ °C/s.

during the heating and cooling of the crystal.⁷ Electron emission from the surface of the crystal can also be modeled using the Fowler–Nordheim equation.^{21,27} Previous work has shown that the pressure of the fill gas can vary the accelerating potential by a factor of 2 (Ref. 28) and that there is an optimum pressure¹² at which a pyroelectric accelerator should be operated.

In the idealized model of a pyroelectric accelerator presented in Fig. 1, we only considered the capacitances of the crystals and the gap. Various other capacitances can be present in the system such as capacitance at the interface between the crystal and the surface to which it is mounted and the capacitance between the crystal face and the vacuum chamber walls. Prior work has²¹ attributed the discrepancy between predicted and experimental values to parasitic capacitance. This explanation worked for the particular case given in Ref. 21 (which required a parasitic capacitance of only 0.8 pF), but it does not scale to larger crystal sizes. For the geometrical dimensions used in our numerical example, the parasitic capacitance would need to be 30 pF in order to cause the observed reduction in potential. (a 1 cm thick, 1 cm radius LiTaO₃ crystal has a capacitance of 12.8 pF and a 1.5 cm thick, 1 cm radius vacuum gap has a capacitance of 0.2 pF, so the parasitic capacitance in the system will be much less than 30 pF). While there is definitely some parasitic capacitance in the system, it will not be large enough to cause the discrepancy between the potential calculated in an idealized model and that attained in a physical system in all cases.

Leakage of charge through both the crystal and gap will cause the potential to be lower than the predicted value. If we use the following solution^{25,26} to Eq. (25a):

$$V = \gamma A R_{eq} \frac{dT}{dt} (1 - e^{-t/(C_{eq} R_{eq})}) \quad (26)$$

The potential for a one-crystal system can be calculated while accounting for charge leakage through both the crystal and the gap. In Fig. 7, we see values for potential versus crystal thickness for a 5×5 mm² rectangular LiTaO₃ crystal, which experienced a temperature change of 50 °C. The idealized calculation [Eq. (5a)] yields values that are higher than those measured experimentally. Accounting for charge leakage [Eq. (26)] using a crystal resistivity of $10^{13} \Omega$ m, a gap

resistance of $8 \times 10^{13} \Omega$, and $dT/dt=0.5 \text{ }^\circ\text{C/s}$ yields values that agree with experiments. We have found that the effect of leakage scales to other geometries as well. It is also worth mentioning that when we state a value for the potential across the gap, this should not be taken to imply that the crystal face is an equipotential surface. Prior work²⁹ has found that the charge may form a ring around the crystal edge resulting in a higher potential at the edge of the crystal than at the center of the crystal surface. When we state a measured value for the potential across the gap, we are referring to the maximum potential; our technique for measuring the potential does not have spatial resolution but rather provides the energy spectrum of the accelerated particles.

V. CONCLUSION

Equations have been presented which can be used to predict the potential and field in an idealized one-crystal pyroelectric accelerator and an extension of this analysis to the two-crystal system is derived. These equations agree with finite element calculations of these quantities for the same idealized systems. When these idealized equations are combined with a simple technique for accounting for charge leakage, the predicted potential agrees well with experimental values. Thermal gradients, charge leakage through the crystal, temperature dependence of material properties, parasitic capacitance, and spontaneous discharges all likely contribute to the (factor of ~ 4) discrepancy between the potential predicted by the idealized model and the measured potential in both the one and two-crystal systems. A more thorough understanding of this interplay is a matter of ongoing investigation.

¹S. B. Lang, *Phys. Today* **58**(8), 31 (2005).

²J. D. Brownridge, *Nature (London)* **358**, 287 (1992).

³J. A. Geuther and Y. Danon, *J. Appl. Phys.* **97**, 104916 (2005).

⁴J. D. Brownridge and S. Raboy, *J. Appl. Phys.* **86**, 640 (1999).

- ⁵J. D. Brownridge and S. M. Shafroth, *Appl. Phys. Lett.* **79**, 3364 (2001).
- ⁶J. D. Brownridge, S. M. Shafroth, D. W. Trott, B. R. Stoner, and W. M. Hooke, *Appl. Phys. Lett.* **78**, 1158 (2001).
- ⁷J. A. Geuther and Y. Danon, *J. Appl. Phys.* **97**, 074109 (2005).
- ⁸E. L. Neidholdt and J. L. Beauchamp, *Anal. Chem.* **79**, 3945 (2007).
- ⁹J. A. Geuther and Y. Danon, *Nucl. Instrum. Methods Phys. Res. B* **261**, 110 (2007).
- ¹⁰B. Naranjo, J. K. Gimzewski, and S. Putterman, *Nature (London)* **434**, 1115 (2005).
- ¹¹J. A. Geuther, Y. Danon, and F. Saglime, *Phys. Rev. Lett.* **96**, 054803 (2006).
- ¹²D. Gillich, A. Kovanen, B. Herman, T. Fullem, and Y. Danon, *Nucl. Instrum. Methods Phys. Res. A* **602**, 306 (2009).
- ¹³D. J. Gillich, R. Teki, T. Z. Fullem, A. Kovanen, E. Blain, D. B. Chrisey, T.-M. Lu, and Y. Danon, *Nanotoday* **4**, 227 (2009).
- ¹⁴G. Rosenman, D. Shur, Ya. E. Krasik, and A. Dunaevsky, *J. Appl. Phys.* **88**, 6109 (2000).
- ¹⁵K. M. Lui, P. S. Leang, Y. K. Kam, and W. M. Lau, *Surf. Interface Anal.* **38**, 957 (2006).
- ¹⁶Y. Watanabe, M. Okano, and A. Masuda, *Phys. Rev. Lett.* **86**, 332 (2001).
- ¹⁷F. Pinto, *Am. J. Phys.* **75**, 513 (2007).
- ¹⁸Comsol Multiphysics version 3.5a, www.comsol.com.
- ¹⁹R. T. Smith, *Appl. Phys. Lett.* **11**, 146 (1967).
- ²⁰A. Kovanen, Y. Danon, and D. Gillich, "X-Ray Production Using Stacked Pyroelectric Crystals," 2008 ANS National Meeting, Anaheim, CA, ANS Transactions Vol. 98, 2008 (unpublished), pp. 406–407.
- ²¹J. A. Geuther, "Radiation generation with pyroelectric crystals," Ph.D. thesis, Rensselaer Polytechnic Institute, 2007.
- ²²Q. Wang, S. Leng, and Y. Yu, *Phys. Status Solidi B* **194**, 661 (1996).
- ²³J. Geuther, Y. Danon, F. Saglime, and B. Sones, "Electron Acceleration for X-ray Production Using Paired Pyroelectric Crystals," Proceedings from the Sixth International Meeting on Nuclear Applications of Accelerator Technology, San Diego, 1–5 June, 2003 (unpublished), p. 124.
- ²⁴S. Longuemart, A. H. Sahraoui, D. Dadarlat, S. Delenclos, C. Kolinsky, and J. M. Buisine, *Rev. Sci. Instrum.* **74**, 805 (2003).
- ²⁵S. B. Lang and F. Steckel, *Rev. Sci. Instrum.* **36**, 929 (1965).
- ²⁶S. B. Lang, S. A. Shaw, L. H. Rice, and K. D. Timmerhaus, *Rev. Sci. Instrum.* **40**, 274 (1969).
- ²⁷R. H. Fowler and L. Nordheim, *Proc. R. Soc. London, Ser. A* **119**, 173 (1928).
- ²⁸J. D. Brownridge and S. M. Shafroth, *Appl. Phys. Lett.* **83**, 1477 (2003).
- ²⁹N. Kukhtarev, J. D. T. Kukhtareva, M. Bayssie, J. Wang, and J. D. Brownridge, *J. Appl. Phys.* **96**, 6794 (2004).